International Journal of Nanotechnology and Application (IJNA)
ISSN(P): 2277-4777; ISSN(E): 2278-9391
Vol. 5, Issue 5, Dec 2015, 1-10

EFFECTS OF ADHESIVE AND INTERPHASE BEHAVIOR OF AA6061/AlN NANOPARTICULATE METAL MATRIX COMPOSITES

A. CHENNAKESAVA REDDY

Professor, Department of Mechanical Engineering, JNTUH College of Engineering, Hyderabad, Telangana, India

ABSTRACT

In this article two types of RVE models have been implemented using finite element analysis. Aluminum nitride nanoparticles were used as a reinforcing material in the matrix of AA6061 aluminum alloy. It has been observed that the nanoparticle did not overload during the transfer of load from the matrix to the nanoparticle via the interphase due to interphase between the nanoparticle and the matrix. The tensile strength and elastic modulus has been found increasing with an increase volume fraction of aluminum nitride in the AA6061/AlN nanocomposites.

KEYWORDS: RVE Models, ALN, Aa6061, Finite Element Analysis, Interphase

Received: Oct 20, 2015; **Accepted:** Oct 26, 2015; **Published:** Nov 02, 2015; **Paper Id.:** IJNADEC20151

Original Article

INTRODUCTION

Aluminum nitride (AlN) nanoparticles are available in high purity with large specific surface area and high surface activity. For composite materials, the aluminum nitride nanoparticles have good interface compatibility, and can enhance the mechanical and electrical properties. AlN is used for manufacturing of metal matrix and polymer matrix composites, mainly in the heat seal adhesives, electronic casing materials and high thermal conductivity ceramics. AA6061 consists of magnesium and silicon as its major alloying elements. AA6061 is commonly used in the construction of aircraft structures, such as wings and fuselages, automotive parts, such as wheel spacers and aluminum cans for the packaging of foodstuffs and beverages.

The higher stiffness of ceramic particles can result in an incremental increase in the stiffness of a composite [1, 2]. Micro reinforced particles in the metal matrix composites can reduce impact resistance. This property can be enhanced by using nanoparticles [3]. The existence of an interphase of higher strength and modulus between the matrix and particle can enhance mechanical properties [4]. Decreasing the interfacial strength can encourage the interfacial debonding of reinforced particulates from the matrix. Interfacial debonding causes shear yield of the matrix. Very small particles are sometimes difficult to disperse, creating clusters that behave as a single big particle [5, 6]. The tensile properties of nanocomposites have been analyzed using micromechanical models. The elastic modulus depends on the interfacial adhesion and the matrix's crystalline structure [7, 8].

The aim of this paper was to establish the effect of presence and absence of interphase as a consequence of with and without wetting criteria of AlN by AA6061 molten metal. The RVE models were used to analyze the AA6061/AlN nanocomposites using finite Element analysis.

STRENGTHENING MECHANISMS

The tensile strength of a particulate composite derives on the strength of the weakest region and metallur-

gical phenomena in it [9, 10]. Even if several theories of composite strength have been available, none is unanimously accepted. Pukanszky et al [11] have presented an empirical relationship for strong particle-matrix interfacial bonding, as given below:

$$\sigma_c = \left[\sigma_m \left(\frac{1-v_p}{1+2.5v_p}\right)\right] e^{Bv_p} \tag{1}$$

where *B* is an empirical constant, which depends on the surface area of particles, particle density and interfacial bonding energy. The value of B varies between from 3.49 to 3.87. This criterion considers the presence of interfacial bonding between the particulate and the matrix. The effect of particle size and voids/porosity are not well thought-out in this criterion.

A new criterion [12, 13] has been formulated by the author considering adhesion, formation of precipitates, particle size, agglomeration, voids/porosity, obstacles to the dislocation, and the interfacial reaction of the particle/matrix. The formula for the strength of composite is given below:

$$\sigma_c = \left[\sigma_m \left\{\frac{1-(v_p+v_v)^{2/3}}{1-1.5(v_{p+}v_v)}\right\}\right] e^{m_{p(v_p+v_v)}} + kd_p^{-1/2} \tag{2}$$

$$k = E_m m_m / E_p m_p$$

where v_v and v_p are the volume fractions of voids/porosity and the nanoparticle in the composite, m_m and m_p are the possion's ratios of the matrix and particulates and d_p is the mean diameter of the nanoparticle.

Elastic modulus (Young's modulus) is a measure of the stiffness of a material. Elastic modulus is constant in all directions for isotropic materials. Ishai and Cohen [14] have developed a relation between moduli of composite and matrix based on a uniform stress applied at the boundary; the ratio of elastic moduli is given by

$$\frac{E_c}{E_m} = 1 + \frac{1+(\delta-1)v_p^{2/3}}{1+(\delta-1)\left(v_p^{2/3}-v_p\right)} \tag{3}$$

which is upper-bound equation. In the derivation of above formula, they assumed that the particle and matrix are in a state of macroscopically homogeneous and the adhesion is perfect at the interface. The lower-bound equation is given by

$$\frac{E_c}{E_m} = 1 + \frac{v_p}{\delta/(\delta-1)-v_p^{1/3}} \tag{4}$$

where $\delta = E_p / E_m$.

The proposed equations [12, 13] by the author to find Young's modulus of composites and interphase including the effect of voids/porosity as given below:

The upper-bound equation is given by

$$\frac{E_c}{E_m} = \left(\frac{1-v_v^{2/3}}{1-v_v^{2/3}+v_v}\right) + \frac{1+(\delta-1)v_p^{2/3}}{1+(\delta-1)(v_p^{2/3}-v_p)} \tag{5}$$

The lower-bound equation is given by

$$\frac{E_c}{E_m} = 1 + \frac{v_p - v_p}{\delta/(\delta-1)-(v_p+v_v)^{1/3}} \quad (6)$$

where, $\delta = E_p/E_m$.

The transverse modulus is given by

$$E_t = \frac{E_m E_p}{E_m + E_p(1-v_p{}^{2/3})/v_p{}^{2/3}} + E_m\left(1 - v_p{}^{2/3} - v_v{}^{2/3}\right) \quad (7)$$

The young's modulus of the interphase is obtained by the following formula:

$$E_i(r) = \left(\alpha E_p - E_m\right)\left(\frac{r_i - r}{r_i - r_p}\right) + E_m \quad (8)$$

MATERIALS AND METHODS

The matrix material was AA6061 aluminum alloy. AA6061 is a precipitation hardening aluminum alloy, containing magnesium and silicon as its major alloying elements. Optical microstructure of AA6061 aluminum alloy is shown in figure 1(a). The reinforcement material was aluminum nitride (AlN) nanoparticles of average size 100nm. The morphology of AlN nanoparticles is spherical, and they appear as a gray powder as shown in figure 1(b). The mechanical properties of materials used in the present work are given in table 1. The tensile specimens were fabricated by the stir casting process [12, 13]. The heat-treated samples were machined to get flat-rectangular specimens (figure 2) for the tensile tests. The tensile test was performed on a Universal Test Machine (UTM) at a specified grip separation and pulled until failure. The test speed was 1 mm/min (as for ASTM D3039). A strain gauge was used to determine elongation. The scanning electron microscope (SEM) was used to determine interphase.

Table 1: Mechanical Properties of AA6061 Matrix and AlN Nanoparticles

Property	AA 6061	AlN
Density, g/cc	2.70	3.26
Elastic modulus, GPa	69.8	330
Ultimate tensile strength, MPa	310	270
Poisson's ratio	0.33	0.24

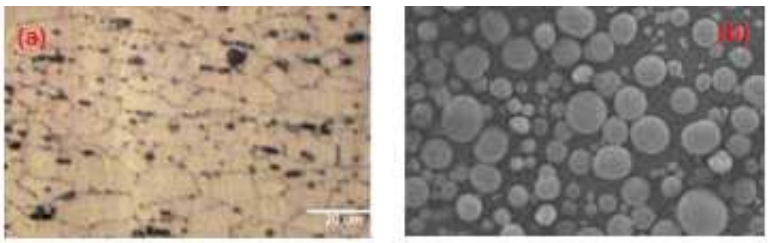

Figure 1: Microstructure of (a) Aa6061 and (b) Morphology of Aluminum Nitride Nanoparticle

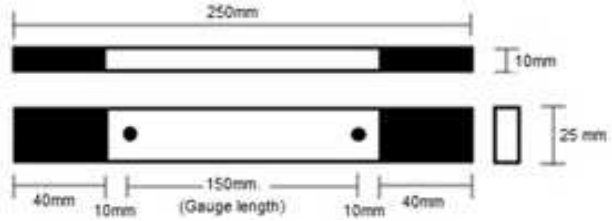

Figure 2: Shape and Dimensions of Tensile Specimen

Finite Element Analysis (FEA)

The finite element analysis has been very efficient in determining the mechanical properties of non-homogeneous materials like composites [15]. In finite element numerical models very fine meshes need to be applied inside and around the interphase layers which results in large number of degrees of freedom. Currently, the use of a representative volume element (RVE) or a unit cell of the composite microstructure, in conjunction with a finite element (FE) analysis tool is well established for examining the effective material properties and understanding the micromechanics of the composite materials [16, 17]. In this research, a cubical RVE was implemented to analyze the tensile behavior AA6061/aluminum nitride nanocomposites (figure 3). The volume fraction of a nanoparticle in the RVE is computed using equation [18]:

$$v_p(\text{RVE}) = \frac{\text{Volume of nanoparticle}}{\text{Volume of RVE}} = \frac{16}{3} \times \left(\frac{\text{r}}{\text{a}}\right)^3 \quad (9)$$

where, *r* represents the nanoparticle radius and *a* specifies the length of the cubical RVE. The volume fraction of the nanoparticles in the nanocomposite (v_p) was selected to be 10%, 20% and 30%; the nanoparticle radius (*r*) was 100 nm.

Two RVE schemes namely: without interphase and with interphase between the matrix and the reinforcement were employed. The loading on the RVE is assumed as symmetric displacement to have equal displacements at both ends. The large strain PLANE183 element was used to mesh the matrix and the interphase zones in the models. COMBIN14 spring-damper element was used to model the adhesion between the interphase and the nanoparticle. The stiffness was assumed to be unity for perfect adhesion. It is essential to set the strain rates of the FEM models based on the experimental tensile tests to converge an exact nonlinear solution. Hence, the ratio of the tensile test speed to the gauge length of the tensile specimen should be equal to the equivalent ratio in the RVE displacement model. As a result, the rate of displacement in the RVEs was considered as 0.1min^{-1}.

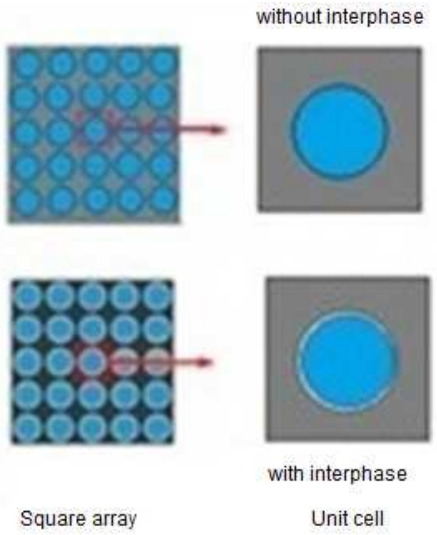

Figure 3: The RVE models

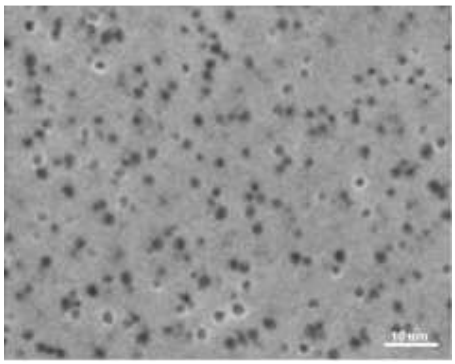

Figure 4: AlN Nanoparticle Distribution in AA6061 Matrix

RESULTS AND DISCUSSIONS

Figure 4 reveals the microstructure of AA6061/AlN nanocomposite. The AlN nanoparticles are distributed in the AA6061 matrix uniformly (approximated). Figure 5 depicts the tensile strengths of the nanocomposites obtained by FEA (RVE model), Pukanszky et al model, AC Reddy model, and experimental procedure. The tensile strength increases with an increase of AlN content in the nanocomposites. Without interphase and bare consideration of adhesive bonding, the de-bonding occurs at the particle/matrix interface region in the nanocomposite as shown in figure 6. It is also observed that the stress induced in the nanoparticle gets increased with the increasing content of AlN in the composite. This indicates the transfer of load from the matrix to the nanoparticle. Figure 7 shows the effect of interphase between the nanoparticle and the matrix on the major principle stress induced in the nanocomposite in the direction of tensile loading. The major principle stress increases with an increase of AlN in the nanocomposite. It can be noticed that the breakage occur between the interphase and the nanoparticle in the composites having low volume fractions 10 to 20%) of AlN. In the composite having 30% volume fraction of AlN, there is an evidence of breakage of bonding not only between the nanoparticle and the interphase but also between the matrix and the interphase. Due to interphase between the nanoparticle and the matrix, the nanoparticle is not overloaded during the transfer of load from the matrix to the nanoparticle via the interphase.

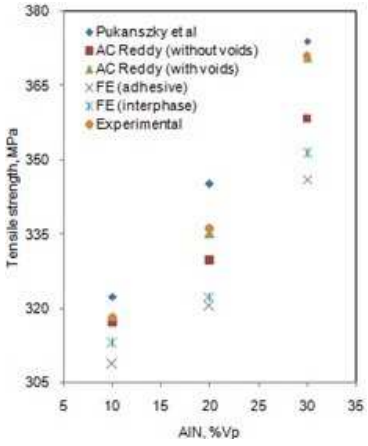

Figure 5: Effect of Volume Fraction on Tensile Strength

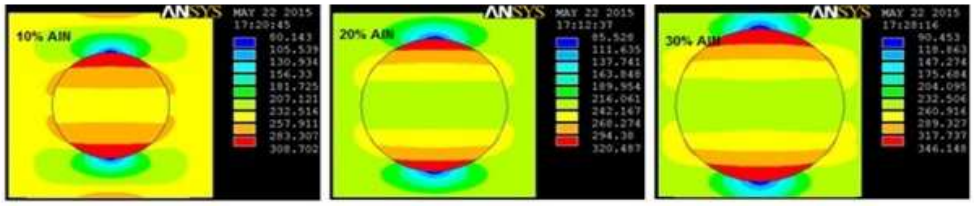

Figure 6: Tensile Stress without Interphase

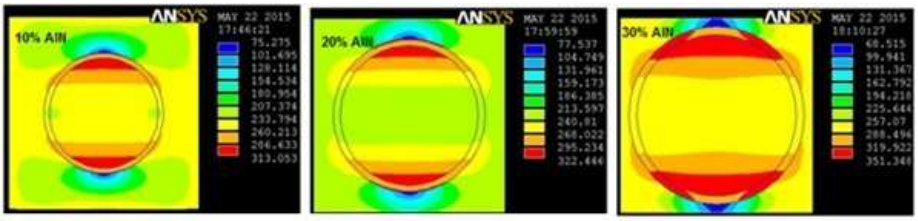

Figure 7: Tensile Stress with Interphase

Pukanszky et al model does not include the effect of voids present in the nanocomposites. AC Reddy model includes the effect of voids present in the nanocomposite. The tensile strengths obtained by AC Reddy model (with voids) and experimental results were less than those obtained from Pukanszky et al model. This may be attributed to the presence of voids in the nanocomposites. In the presence of voids in the nanocomposite, the interface region between the nanoparticle and the matrix gets stiffened and consequently this leads the slow rate of increasing (or remain constant) the tensile strength with an increase in the nanoparticles content. Results obtained from AC Reddy model were nearly equal to the experimental values. On the other hand, the deviations of FEA (RVE model) results with the experimental results possibly occur as a result of micro-metallurgical factors (such as the formation of voids and nanoparticle clustering) that were not considered in the RVE models. However, the nonlinear deformation behavior of the reinforcements and the matrix/reinforcement debonding were considered in the RVE models. These micromechanical factors might play an important role in the large plastic deformation regime.

Figure 8 shows the elastic strain contours of the RVE models for the situation involving without interphase and with interphase. According to figure 9, the RVE is expanded elastically away from the particle in the direction of the tensile loading. This increases the contact area between the particle and the matrix in the perpendicular direction to the tensile loading and decreases the contact area between the particle and the matrix in the direction of the tensile loading. In addition, the deformation is propagated in the normal direction to the tensile loading. The same kind of trend was observed with the nanocomposites consisting of 10% and 20% AlN.

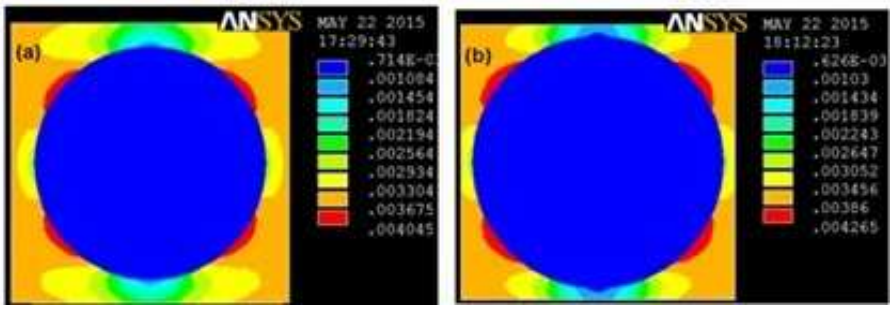

Figure 8: Elastic Strain in the Direction of Tensile Loading: (a) without Interphase And (b) With Interphase For 30%Aln.

Table 2 gives the elastic (tensile) moduli of the nanocomposites obtained by the Rule of Mixtures, Ishai and Cohen model and AC Reddy model with respect to the volume fraction of AlN nanoparticles. By increasing the nanoparticles, the elastic modulus increases appreciably. The results provided by Ishai and Cohen model and AC Reddy model were closer results than the results achieved by the Rule of Mixture. This is due to the existence of voids in the nanocomposites.

Table 2: Elastic Modulus Obtained from Models

Model	Elastic Modulus, GPa		
	10% Vp	20% Vp	30% Vp
Ishai and Cohen	169.90	177.34	184.78
Rule of Mixture	88.05	93.36	98.68
AC Reddy	168.43	175.38	182.31

Figure 9 shows the variation of von Mises stress in the nanocomposite without interphase. The von Mises stress increases with an increase in the volume fraction of AlN. The quality of adhesion at the interface is of crucial importance for the behavior of nanocomposites. The adhesion strength at the interface identifies the load-transfer between the components. Effective stress transfer is the most important thing factor which contributes to the strength of two-phase composite materials. For poorly bonded particles, the stress transfer at the particle/matrix interface is inefficient. Discontinuity in the form of debonding exists because of non-adherence of particles to matrix. However, for composites containing well-bonded particles, addition of particles to a matrix will lead to an increase in strength especially for nanoparticles with high surface areas. It is observed from figure 9 that the debonding occurs at the entire periphery of the nanoparticle without interphase between the nanoparticle and the matrix. Hence, the stress transfer from the matrix to the nanoparticle becomes less for the nanocomposites without interphase. It is noticed from figure 10 that the debonding occurs at the partial periphery of the nanoparticle with interphase between the nanoparticle and the matrix. Hence, the stress transfer from the matrix to the nanoparticle becomes high for the nanocomposites with interphase. The SEM images shown in figure 11 reveal the uniform distribution of AlN nanoparticles (30% Vp). It is also observed the tear bands (figure 11) on the periphery of AlN nanoparticle due to transfer of the shear stress from the matrix to the AlN nanoparticle.

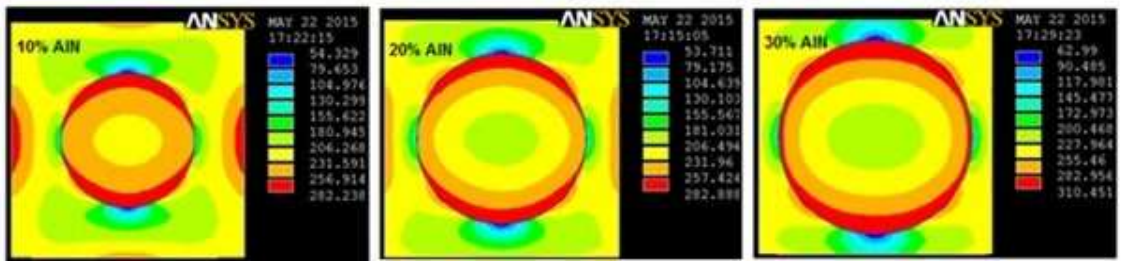

Figure 9: Von Mises Stress without Interphase.

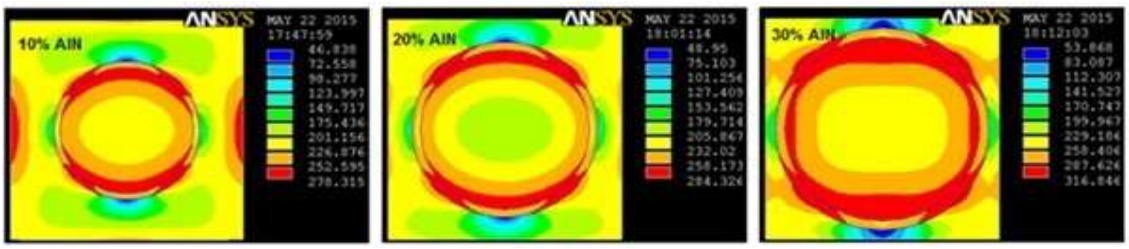

Figure 10: Von Mises Stress with Interphase

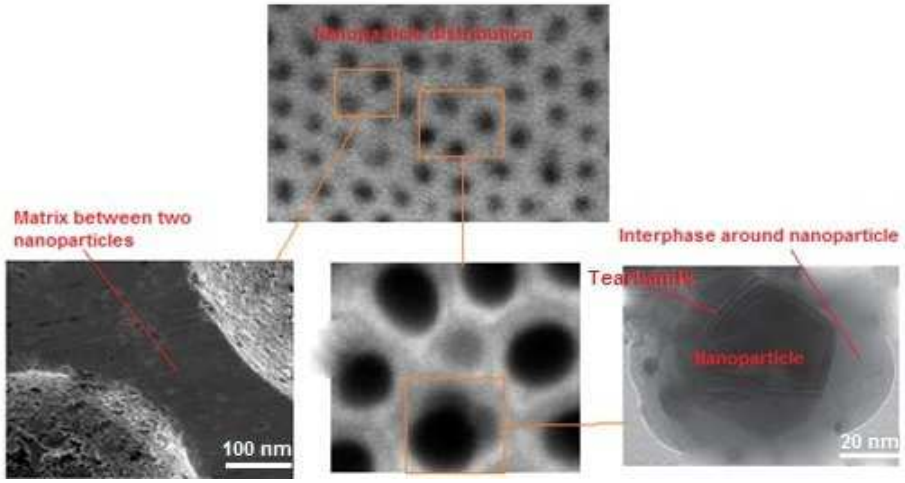

Figure 11: Nanoparticle Distribution and Interphase around Nanoparticle in the Nanocomposite (30% Aln)

The stress concentration around the nanoparticle can be observed from figure 12. It is observed that the interfacial debonding is high between the particle and the matrix because of local stress concentration around the nanoparticle. Plastic flows are initiated within the matrix and ended at the nanoparticle/matrix interface. Owing to the high stress of the nanoparticles, the plastic deformation becomes concentrated at several locations in the matrix. The localized strain is observed around the particle because of the high load transfer effect in particles. The plastic behavior differs considerably with inclusion of interphase between the nanoparticle and the matrix. As the pressure is increased on the RVE model, the plastic strain zone expanded, resulting in a plastic deformation of the interphase between the nanoparticle and the matrix. In the present work, the interphase is softer than the matrix and the nanoparticle and the nanoparticle is stiffer than the matrix. The elastic moduli (stiffness) of AlN nanoparticle and AA6061 matrix are 330 GPa and 69.8 GPa, respectively.

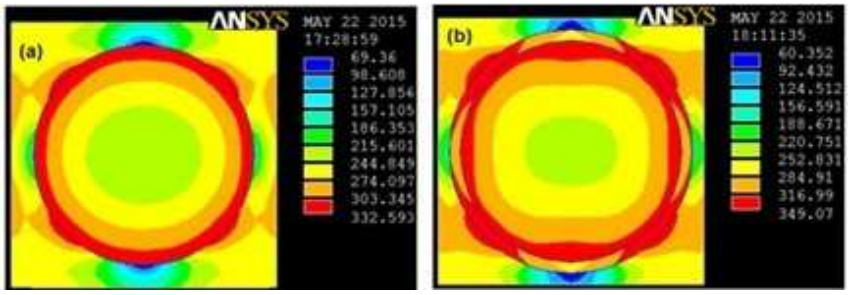

Figure 12: Stress Intensity: (a) Without Interphase and (b) With Interphase For 30%Aln/AA6061 Nanocomposite

CONCLUSIONS

The RVE models give the trend of phenomenon happening in the nanocomposites. Without interphase and barely consideration of adhesive bonding, the debonding occurs at the particle/matrix interface region in the nanocomposite. Due to interphase between the nanoparticle and the matrix, the nanoparticle is not overloaded during the transfer of load from the matrix to the nanoparticle via the interphase. The tensile strengths obtained by AC Reddy model (with voids) and experimental results were lower than those obtained from Pukanszky et al model. . In the case of nanocomposites with interphase between the nanoparticle and the matrix, the stress is transferred through shear from the matrix to the particles. The tensile strength and elastic modulus increases with an increase volume fraction of aluminum nitride in the AA6061/AlN nanocomposites.

ACKNOWLEDGEMENTS

The author thanks the University Grants Commission (UGC), New Delhi for sanctioning this major project. The author also thanks the Officials of Central University, Hyderabad for providing the several SEM images to track interphase between the matrix and the nanoparticle.

REFERENCES

1. *Chennakesava Reddy, A. (2009). Mechanical properties and fracture behavior of 6061/SiCp Metal Matrix Composites Fabricated by Low Pressure Die Casting Process. Journal of Manufacturing Technology Research, 1(3/4), 273-286.*
2. *Chennakesava Reddy, A. & Essa Zitoun. (2011). Tensile properties and fracture behavior of 6061/Al_2O_3 metal matrix composites fabricated by low pressure die casting process. International Journal of Materials Sciences, 6(2), 147-157.*
3. *Friedrich, K., Zhang, Z., & Schlarb, A.K. (2005). Effects of various fillers on the sliding wear of polymer composites. Composites Science and Technology, 65, 2329-2343.*
4. *Romanowicz, M. (2010). Progressive failure analysis of unidirectional fiber-reinforced polymers with inhomogeneous interphase and randomly distributed fibers under transverse tensile loading. Composites part A, 41, 1829-1838.*
5. *Thio, Y.S., Argon, A.S., Cohen, R.E., & Weinberg, M. (2002). Toughening of Isotactic Polypropylene with $CaCO_3$ Particles. Polymer, 43, 3661-3674.*
6. *Chennakesava Reddy, A. (2004). Analysis of the Relationship between the Interface Structure and the Strength of Carbon-Aluminum Composites. NATCON-ME, Bangalore, 61-62.*
7. *Wang, K., Wu, J., Ye, L., & Zeng, H. (2003). Mechanical properties and toughening mechanisms of polypropylene/barium sulfate composites. Composites: Part A, 34, 1199-1205.*
8. *Chennakesava Reddy, A. (2004). Experimental evaluation of elastic lattice strains in the discontinuously SiC reinforced Al-alloy composites. National Conference on Emerging Trends in Mechanical Engineering, Nagpur.*
9. *Chennakesava Reddy, A. (2011). Influence of strain rate and temperature on superplastic behavior of sinter forged Al6061/SiC metal matrix composites, International Journal of Engineering Research & Technology, 4(2), 189-198.*
10. *Chennakesava Reddy, A. & Kotiveerachari, B. (2011). Influence of microstructural changes caused by ageing on wear behaviour of Al6061/SiC composites. Journal of Metallurgy & Materials Science, 53(1), 31-39.*
11. *Punkanszky, B., Turcsanyi, B. & Tudos, F. (1988). Effect of interfacial interaction on the tensile yield stress of polymer composites. In: H. Ishida, editor, Interfaces in polymer, ceramic and metal matrix composites, Amsterdam: Elsevier, 467.*
12. *Chennakesava Reddy, A. (2015). Cause and Catastrophe of Strengthening Mechanisms in 6061/Al2O3 Composites Prepared by Stir Casting Process and Validation Using FEA. International Journal of Science and Research, 4(2), 1272-1281.*
13. *Chennakesava Reddy, A. (2015). Influence of Particle Size, Precipitates, Particle Cracking, Porosity and Clustering of Particles on Tensile Strength of 6061/SiCp Metal Matrix Composites and Validation Using FEA. International Journal of Material Sciences and Manufacturing Engineering, 42(1), 1176-1186.*
14. *Ishai, O., & Cohen, I.J. (1967). Elastic properties of filled and porous epoxy composites. International Journal of Mechanical Sciences, 9, 539-546.*
15. *Chennakesava Reddy, A. (2004). Finite element analysis of elastic-plastic and tensile damage response in carbon-carbon composites under vehicular crush conditions, National Conference on Emerging Trends in Mechanical Engineering, Nagpur.*

16. *Kari, S., Berger, H., & Gabbert, U. (2007). Numerical evaluation of effective material properties of randomly distributed short cylindrical fiber composites. Computational Materials Science, 39, 198-204.*
17. *Duschlbauer, D., Bohm, H.J., & Pettermann, H.E. (2011). Modeling Interfacial Effects on the Thermal Conduction Behavior of Short Fiber Reinforced Composites. International Journal of Materials Research, 6, 717-726.*
18. *Hill, R. (1963), Elastic properties of reinforced solids: some theoretical principles. Journal of the Mechanics and Physics of Solids, 11 (5), 357–372.*